Supporting Information for:

Critical slowing down anticipates emergence and elimination of measles

Andrew T. Tredennick, Eamon O'Dea, TBD, Pejman Rohani, John M. Drake

2020-08-29

S1. Demographic data used in model fitting

We used two sources of demographic data to help constrain model fitting: total population size (N) and birth rate (μ). Both sets of data are reported on an annual basis. To incorporate the data in our model, we fit splines through the annual observations to interpolate daily values (figure S1). Note that the daily interpolated birth rate is still in units of "per year," which is why births are modeled as $\mu N \times dt$ to include the effect of the daily time step dt.
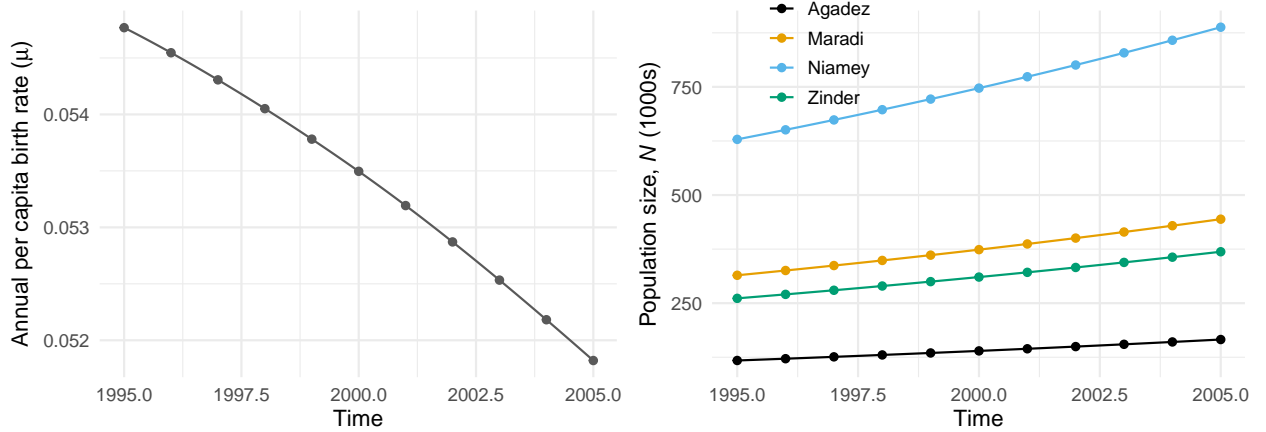

Figure S1: Plots of the demographic data used for model fitting. The points are the actual data and the lines are the interpolated spline fits. Population data is at the disrict level, meaning we have different data for each focal city. Birth rate data is national, meaning each city shares the same birth rates.

S2. Stochastic simulations from the fitted models

Here we show stochastic simulations from the fitted models (figure S2). Simulations are all initialized from the same initial conditions, which were estimated as part of model fitting.
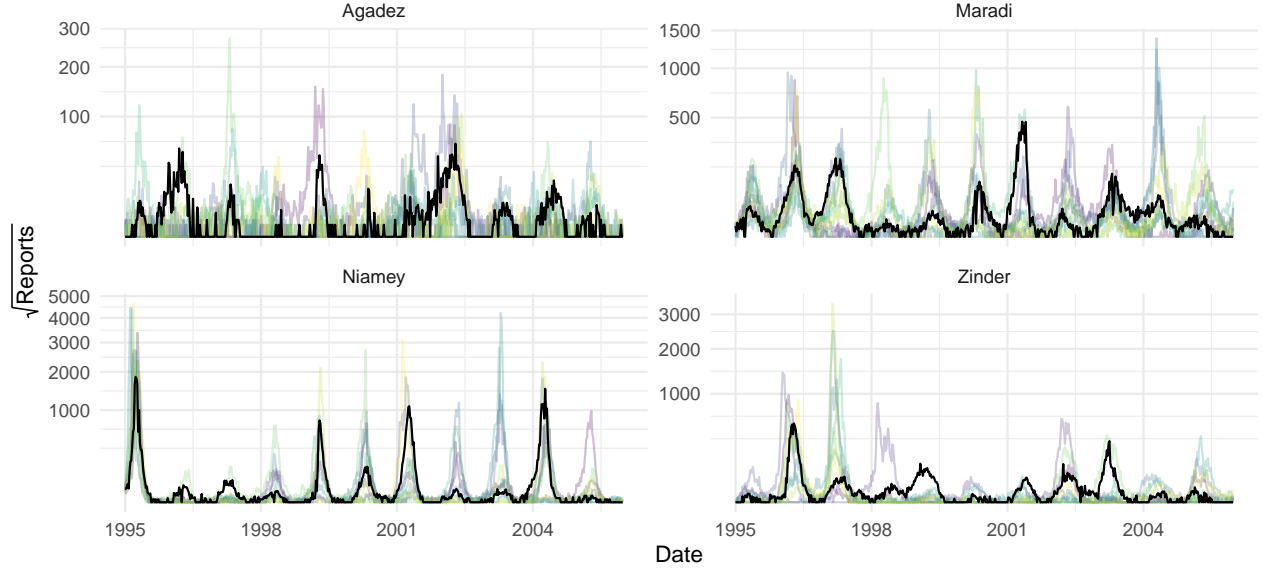
Figure S2: Stochastic simulations from the fitted models. Each colored line is a single realization of the model from the same initial conditions. Ten simulations are shown. The black lines are the observed data. We do not expect model simulations to perfectly align with the data because of the multiple sources of stochasticity present. Thus, these simulations should be judged by their ability to reproduce dynamical features of the data.

S3. Comparisons with benchmarking models

Here we compare our fitted *SEIR* models to two non-mechanistic benchmarking models. Doing so allows us to gain some intuition as to whether accounting for mechanism (i.e., transmission dynamics) improves model fit and eventual inference. The first benchmarking model is a negative binomial sampling model (NBM) that simply assumes all observations are independent and identically distributed. The second benchmarking model is a seasonal moving average model (SARIMA) that can account for data dependencies and seasonal periodicity. Beating the SARIMA is a harder test than beating the NBM.

We fitted both models to the weekly case count observations for each city using maximum likelihood. After fitting, we calculated Akaike's Information Criterion for each model as: $\text{AIC} = 2k - 2\ln(L)$, where k is the number of estimated parameters in the model and L is the model's likelihood. The NBM model has 2 parameters, the SARIMA model has 7 parameters, and the SEIR model has 14 parameters. The results in table S1 show the AIC values for each model. The AIC values for the *SEIR* models are lowest for all cities, suggesting that the addition of mechanism via explicit disease transmission dynamics substantially improves model fit.

Table S1: AIC values for the benchmarking and SEIR models.

City	Neg. Binomial	SARIMA	SEIR
Agadez	2463	2008	1949
Maradi	4618	3545	3521
Niamey	4112	3183	2937
Zinder	3958	2900	2859

S4. Long-run simulations from the fitted the SEIR models

For fitting the SEIR model, we used known population size interpolated between years. This meant we were able to ignore certain demographic processes. For example, we ignored deaths from the susceptible pool under the assumption that the infection rate was much faster than death rate. We also ignored the recovered class completely because their dynamics, outside of the contribution to population size (which we assumed to be known), do not impact the $S, E,$ or I compartments. However, we needed to include births and deaths from all compartments, including R, when simulating the model over arbitrarily long time periods that do not necessarily represent real times for which we would have information on population size.

We added a few terms to the *SEIR* model presented in the main text to account for births and deaths in all compartments. Our strategy was to simulate a population at a dynamic equilibrium, where total population was neither increasing or decreasing over time, but it does fluctuate. Our *simulating model* (in contrast to the *fitting model* in the main text) is as follows.

As in the main text, the *SEIR* model is specified as a set of difference equations,

$$S_{t+dt} - S_t = n_{0S,t} - n_{SE,t} - n_{S0,t} \tag{S.1}$$
$$E_{t+dt} - E_t = n_{SE,t} - n_{EI,t} - n_{E0,t} \tag{S.2}$$
$$I_{t+dt} - I_t = n_{EI,t} + n_{0I,t} - n_{IR,t} - n_{I0,t} \tag{S.3}$$
$$R_{t+dt} - R_t = n_{0R,t} + n_{IR,t} - n_{R0,t}, \tag{S.4}$$

where $\mathbf{n}_t$ are random variables representing the number of individuals transitioning into or out of each class at each update $t \rightarrow t + dt$. Transition definitions are in Table S2.

Table S2: Transitions in the simulating model.

Random variable	Transition	$(\Delta S, \Delta E, \Delta I, \Delta R)$
n_{0S}	Births into the S compartment, not vaccinated	(1, 0, 0, 0)
n_{SE}	Number of people transitioning from S to E	(-1, 1, 0, 0)
n_{SO}	Number of deaths leaving S	(-1, 0, 0, 0)
n_{EI}	Number of people transitioning from E to I	(0, -1, 1, 0)
n_{E0}	Number of deaths leaving E	(0, -1, 0, 0)
n_{0I}	Number of imported infections	(0, 0, 1, 0)
n_{IR}	Number of people transitioning from I to R	(0, 0, -1, 1)
n_{I0}	Number of deaths leaving I	(0, 0, -1, 0)
n_{0R}	Births into the R compartment, vaccinated	(0, 0, 0, 1)
n_{R0}	Number of deaths leaving R	(0, 0, 0, -1)

The stochastic random variables are specified as follows:

$$n_{0S,t} \sim \text{Poisson}((1-p)\mu N_t \times dt) \tag{S.5}$$
$$(n_{SE,t}, n_{S0,t}) \sim \text{Mult}(S_t, (\lambda_{SE,t}, \lambda_{d,t})) \tag{S.6}$$
$$(n_{EI,t}, n_{E0,t}) \sim \text{Mult}(E_t, (\lambda_{EI,t}, \lambda_{d,t})) \tag{S.7}$$
$$(n_{IR,t}, n_{I0,t}) \sim \text{Mult}(I_t, (\lambda_{IR,t}, \lambda_{d,t})) \tag{S.8}$$
$$n_{I0,t} \sim \text{Poisson}(\psi \times dt) \tag{S.9}$$
$$n_{0R,t} \sim \text{Poisson}(p\mu N_t \times dt) \tag{S.10}$$
$$n_{R0,t} \sim \text{Binomial}(R_t, \lambda_{d,t}), \tag{S.11}$$

where p is the vaccination coverage (set at $p = 0.7$), μ is the constant birth rate (set at $\mu = 0.05$), ψ is the rate of imported infections (estimated by the model), and λ_d, λ_{SE}, λ_{EI}, and λ_{IR} are the probabilities of death, exposure, becoming infectious, and recovery, respectively. These probabilities are modeled as:

$$\lambda_{d,t} = 1 - e^{-\nu N_t dt} \tag{S.12}$$

$$\lambda_{SE,t} = 1 - e^{-\frac{\beta_t I_t dt}{N_t}} \tag{S.13}$$

$$\lambda_{EI,t} = 1 - e^{-\eta E_t dt} \tag{S.14}$$

$$\lambda_{IR,t} = 1 - e^{-\gamma I_t dt} \tag{S.15}$$

where β_t is a time-varying rate of transmission, η is a time-invariant rate from the exposed class to the infectious class, γ is a time-invariant recovery rate, and ν is the constant death rate. We set $1/\eta = 8$ days, $1/\gamma = 5$ days, and $\nu = 0.05$. We used a daily time step of $dt = year/365$. Recall that we set birth rate equal to death rate ($\nu = \mu = 0.05$) to achieve a relatively constant equilibrium population size. We modeled the rate of transmission as:

$$\beta_t = \beta \left(1 + \exp \left(\sum_{i=1}^{6} q_i \xi_{i_t} \right) \right) \Gamma_t. \tag{S.16}$$

β is the mean transmission rate and the term $\sum_{i=1}^{6} q_i \xi_{i_t}$ is a B-spline to model seasonality in transmission. The B-spline bases (ξ_{i_t}) are periodic with a 1 year period. The transmission rate (β_t) is also subject to stochastic process noise at each time step, Γ_t, which we model as gamma-distributed white (temporally uncorrelated) noise with mean 1 and intensity σ^2 [1].

Finally, observations were simulated from the model on a weekly time step by drawing counts of cases (y_t) from a negative binomial distribution centered on the number of people that transitioned from the infectious to recovered class over seven days (x_t), subject to estimated reporting rate (ρ), and with a dispersion parameter equal to the MLE: $y_t \sim \text{Negative Binomial}(\rho x_t, \tau)$.

In this model, the effective reproduction number can be approximated as:

$$R_E(t) \approx \frac{S_t}{N_t} \frac{\eta \beta_t}{(\eta + \nu)(\gamma + \nu)}.$$

The model described above was implemented in the R package pomp [2,3] to simulate the re-emergence and elimination scenarios.

S5. Computing the time of critical transitions

To define the null and test intervals for our simulations of re-emergence and elimination, we need to know when the critical transition between alternative modes of fluctuation occurs. For re-emergence, we defined the year of the critical transition as the year just after the effective reproduction number (R_E) reaches or exceeds the critical value of 1. For example, if R_E reaches or exceeds 1 at some point during the fifth year of the simulation, then the critical transition year is defined as the sixth year of the simulation. Thus, the simulated data for calculating early warning signals ends at the end of the fifth year. We call this year the "critical year." When determining the critical year, we eliminate the variation in R_E that arises from the gamma white noise factor and thus calculate the expected value of $R_E(t)$ over the set of all simulation replicates at time t. From the full window ranging from the beginning of the simulation to the end of the critical year, we defined the null interval as the first half of the window (far from $R_E = 1$) and the test interval as the second half of the full window (near $R_E = 1$). Figure S3 shows a typical example.
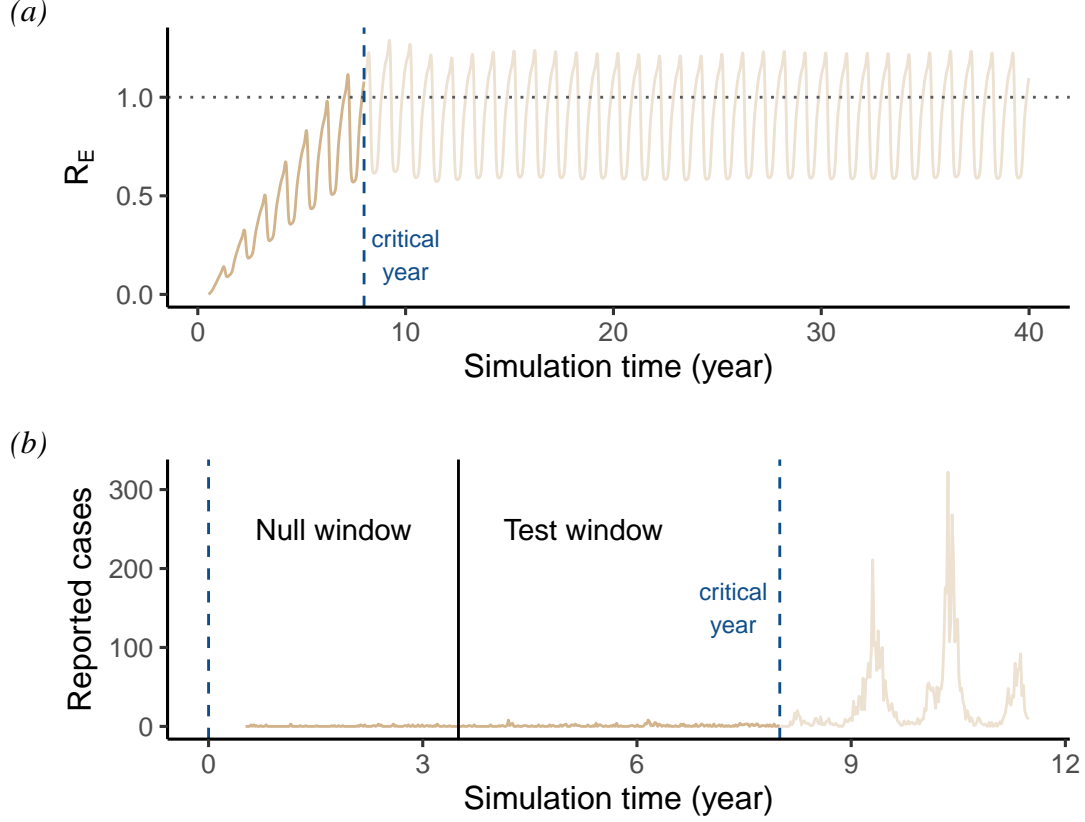
Figure S3: A typical emergence simulation for Maradi where the initial number of susceptibles was scaled by 1e-04. (*a*) The simulated trajectory of R_E and the year in which R_E first reaches the critical value of 1 (denoted by dashed blue line). (*b*) The simulated trajectory of the number of cases. Note that the x-axis has been reduced relative to the top panel. The two vertical blue lines indicate the start (left-most line) and end (line for critical year) of the full window. The black line demarcates the division between the equal-length null and test intervals.

For simulations of disease elimination by increasing the vaccination coverage of the population, we define the critical time as the time at which vaccination coverage reaches the threshold needed for herd immunity. This vaccination threshold is defined as $p = 1 - 1/R_0$. Because our transmission function is seasonal, we first aproximated time-specific R_0 as: $R_0(t) = \frac{\eta \beta_t}{(\eta+\nu)(\gamma+\nu)}$, where $1/\eta$ is the incubation period, $1/\gamma$ is the infectious period, β_t is the time-specific rate of transmission, and ν is the death rate. Only β_t is estimated by our model. We set $1/\eta = 8$ days, $1/\gamma = 5$ days, and $\nu = 0.05$ per year. Figure 2 in the main text shows our estimates of R_0 over the course of a year using this approximation. We took a conservative approach for calculating the vaccination threshold by using the maximum value of $R_0(t)$ out of the range of values in its seasonal variation. That is, we set $p = 1 - 1/\max(R_0(t))$. We set the time at which vaccination coverage is equal to p as the endpoint for the EWS analysis. All elimination simulations had vaccination campaigns that started at year 50. So, we define the test interval as the times between the beginning of year 50 and the year at which vaccination coverage is equal to p. We then defined the null interval as a window with length equal to the test interval and ending at end of year 49. Figure S4 shows a typical example.
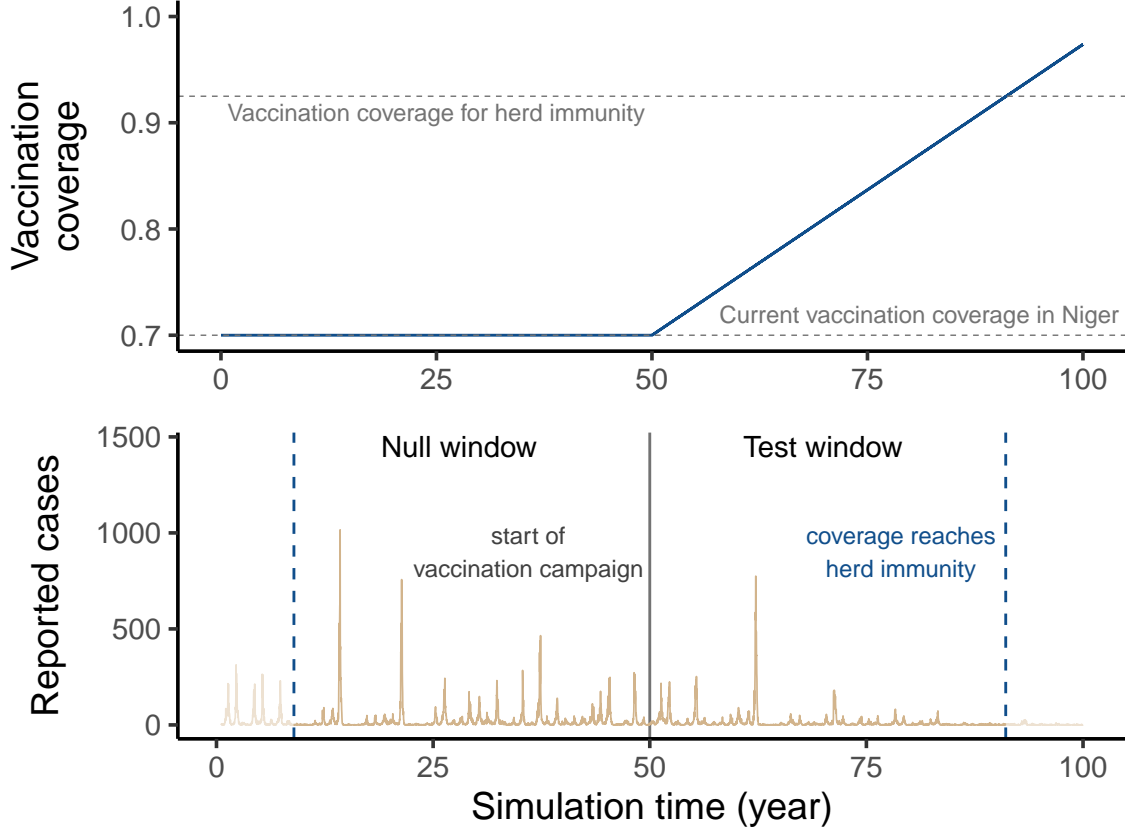
Figure S4: A typical elimination simulation for Maradi where the rate to full vaccination coverage is 1.5e-05 per day. The null and test intervals are defined based on the time at which the vaccination campaign begins (year 50, black line) and the year at which vaccination coverage reaches the vaccination threshold for herd immunity (right-most dashed blue line). The beginning of the null interval is determined by the length of the series from time 50 to the time of herd immunity: the null interval ends at time 50 (when vaccination campaign begins) and starts at whatever time results in a series that is equal in length to the test interval.

S6. Early warning signals

We calculated nine early warning signals using the `spaero::get_stats()` function. Formulas for the early warning signals are in table S1.

Table S3: List of candidate early warning signals and their estimating equations. Note that b denotes the bandwidth. See [4] for details.

EWS	Estimator	Theoretical Correlation with $R_E(t)$ in an emergence scenario
Mean	$\bar{y} = \sum_{i=1}^{n} \frac{y_i}{n}$	Positive
Variance	$s^2 = \sum_{i=1}^{n} \frac{(y_i - \bar{y})^2}{n}$	Positive
Coefficient of variation	$\frac{s}{\bar{y}}$	Null
Index of dispersion	$\frac{s^2}{\bar{y}}$	Positive
Skewness	$\frac{1}{s^3} \sum_{i=1}^{n} \frac{(y_i - \bar{y})^3}{n}$	Positive
Kurtosis	$\frac{1}{s^4} \sum_{i=1}^{n} \frac{(y_i - \bar{y})^4}{n}$	Positive
Autocovariance	$s_1^2 = \sum_{i=2}^{n} \frac{(y_i - \bar{y})(y_{i-1} - \bar{y})}{n}$	Positive

EWS	Estimator	Theoretical Correlation with $R_E(t)$ in an emergence scenario
Autocorrelation	$r_1 = \frac{s_1^2}{s^2}$	Positive
Decay time	$-1/\ln(r_1)$	Positive

S7. Trends of early warning signals

Theory suggests that most EWS should increase as disease dynamics approach a critical transition from below (emergence). When approaching the critical transition from above (elimination), a simple linear noise approximation to the SEIR model dynamics leads to the prediction that the mean and variance should decrease while the autocorrelation should develop a longer period.

To confirm that the EWS are behaving as expected, and to document cases in which they do not, we plotted histograms of the EWS for the test and null intervals for both simulation types, emergence and elimination.
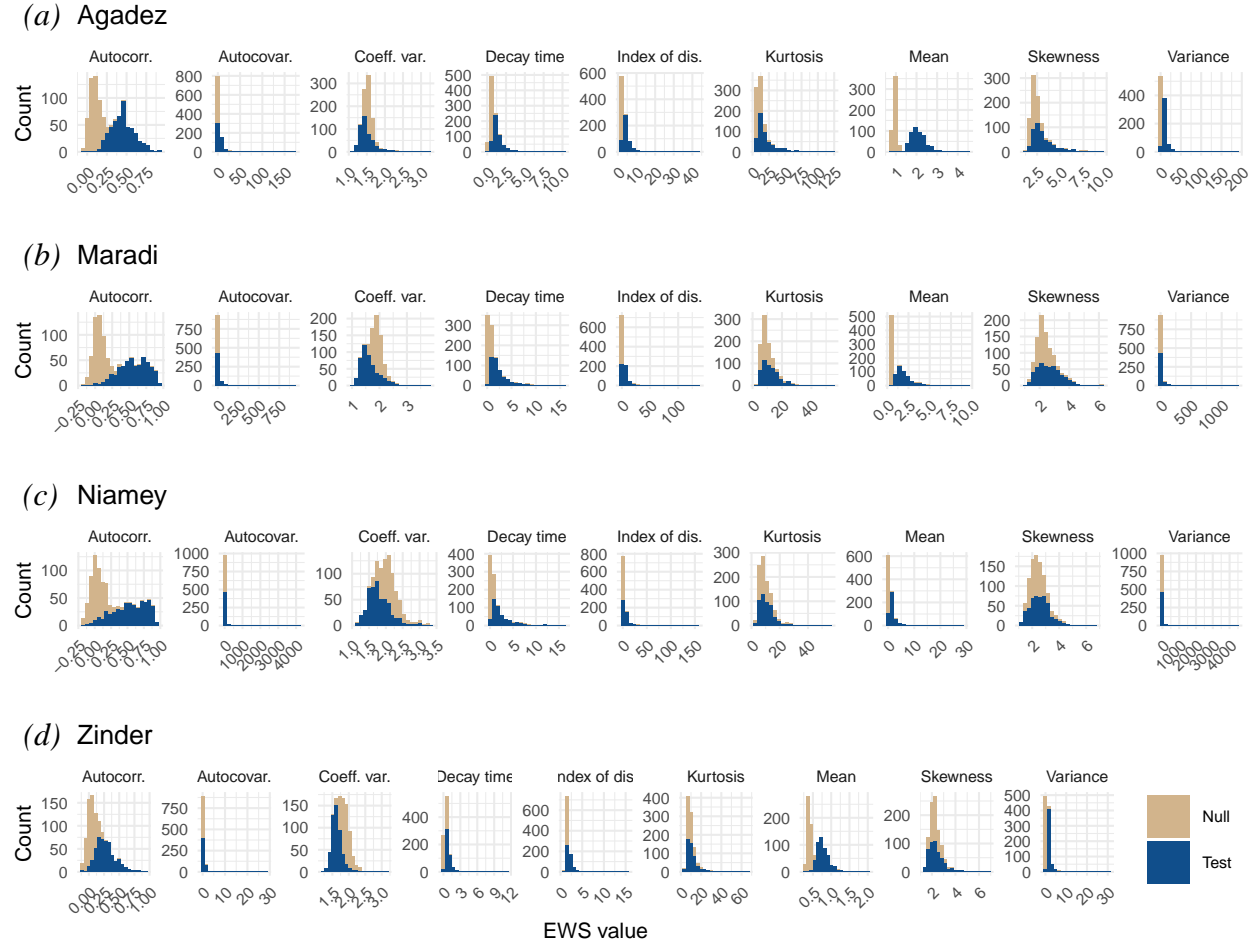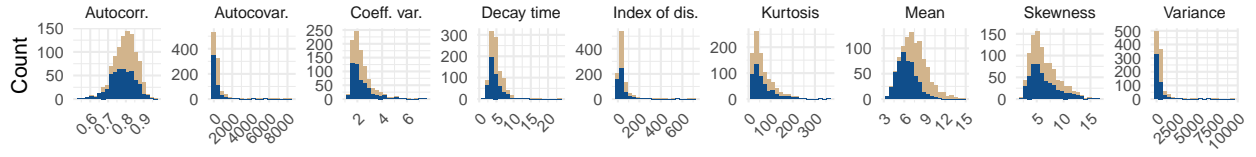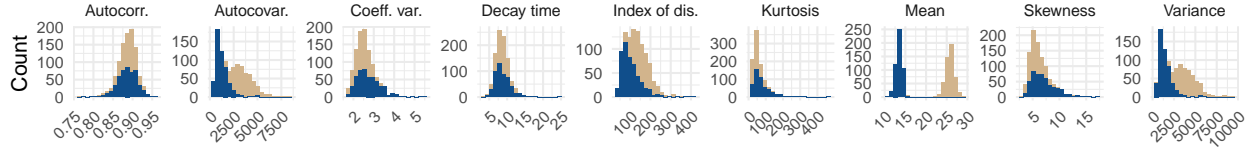

Figure S5: Histograms of EWS from emergence simulations where susceptible depletion fraction was 1e-04.
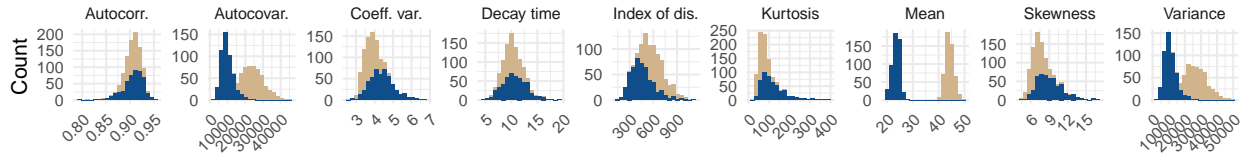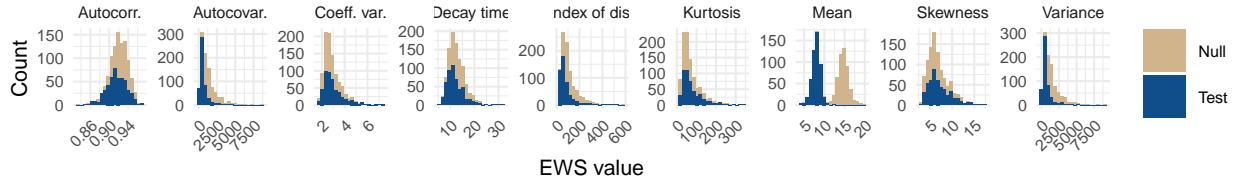
(a) Agadez

(b) Maradi

(c) Niamey

(d) Zinder

EWS value

Figure S6: Histograms of EWS from elimination simulations where rate of vaccination coverage reaching 1 is 1.5e-05.

S8. Bootstrapped parameter confidence intervals

We used a bootstrap approach to estimate approximate 95% confidence intervals for all parameters. Below we show summary statistics for all parameters except the B-splines. For B-splines, and transmission rate more generally, we plot the seasonal transmission rate function for all bootstrap replicates (Figure S7).

Table S4: Maximum likelihood estimates and summary statistics of parameters from bootstrapped estimates for Agadez.

Parameter	MLE	Mean	Median	SD	Lower 95% CI	Upper 95% CI
Log likelihood	-961	NA	NA	NA	NA	NA
Log likelihood S.E.	0.114	NA	NA	NA	NA	NA
β	171	187	165	110	43	467
σ	0.0968	0.081	0.0869	0.0327	0.00123	0.133
ψ	7.8	8.71	8.42	2.33	5.14	13.7
ρ	0.77	0.759	0.756	0.166	0.474	0.999
τ	0.107	0.115	0.11	0.0479	0.0426	0.235
$S_{t=0}$	0.23	0.237	0.205	0.166	0.0138	0.736
$E_{t=0}$	5.53e-06	1.75e-05	1.08e-05	1.66e-05	2.53e-06	6.67e-05
$I_{t=0}$	1.2e-05	9.34e-06	6.94e-06	7.84e-06	1.87e-06	2.94e-05

Table S5: Maximum likelihood estimates and summary statistics of parameters from bootstrapped estimates for Maradi.

Parameter	MLE	Mean	Median	SD	Lower 95% CI	Upper 95% CI
Log likelihood	-1750	NA	NA	NA	NA	NA
Log likelihood S.E.	0.155	NA	NA	NA	NA	NA
β	483	533	529	131	319	813
σ	0.0557	0.0518	0.0518	0.0118	0.0316	0.0729
ψ	24.9	29.7	27.3	10.6	14.9	57.1
ρ	0.333	0.333	0.333	0.0261	0.292	0.387
τ	0.0769	0.0801	0.0805	0.0166	0.054	0.113
$S_{t=0}$	0.104	0.0961	0.0968	0.0172	0.0673	0.13
$E_{t=0}$	8.08e-06	4.01e-05	3.21e-05	3.17e-05	4.13e-06	0.000114
$I_{t=0}$	3.35e-05	2.46e-05	1.92e-05	1.79e-05	3.78e-06	6.84e-05

Table S6: Maximum likelihood estimates and summary statistics of parameters from bootstrapped estimates for Niamey.

Parameter	MLE	Mean	Median	SD	Lower 95% CI	Upper 95% CI
Log likelihood	-1450	NA	NA	NA	NA	NA
Log likelihood S.E.	0.154	NA	NA	NA	NA	NA
β	371	360	374	119	11.2	560
σ	0.0887	0.0818	0.0819	0.0146	0.0594	0.116
ψ	23.3	24.8	24.4	5.14	15.8	35.2
ρ	0.262	0.262	0.255	0.0254	0.219	0.315
τ	0.0526	0.0522	0.0518	0.0132	0.0279	0.0784
$S_{t=0}$	0.11	0.112	0.113	0.0124	0.0897	0.136
$E_{t=0}$	0.000119	0.00024	0.000185	0.000216	1.7e-05	0.000783
$I_{t=0}$	0.000134	0.000111	9.72e-05	7.64e-05	1.74e-05	0.000297

Table S7: Maximum likelihood estimates and summary statistics of parameters from bootstrapped estimates for Zinder.

| Parameter	MLE	Mean	Median	SD	Lower 95% CI	Upper 95% CI
Log likelihood	-1420	NA	NA	NA	NA	NA
Log likelihood S.E.	0.0903	NA	NA	NA	NA	NA
β	180	223	214	98.6	78	445
σ	0.0757	0.0682	0.0695	0.0176	0.0269	0.0969
ψ	10.5	11.6	10.9	4.41	5.83	18.9
ρ	0.364	0.346	0.35	0.0727	0.226	0.486
τ	0.0351	0.0394	0.0369	0.0164	0.0167	0.0813
$S_{t=0}$	0.222	0.237	0.222	0.0921	0.116	0.481
$E_{t=0}$	1.19e-06	3.67e-06	1.84e-06	4.48e-06	6.29e-07	1.32e-05
$I_{t=0}$	9.23e-07	2.16e-06	1.54e-06	1.65e-06	5.03e-07	5.84e-06
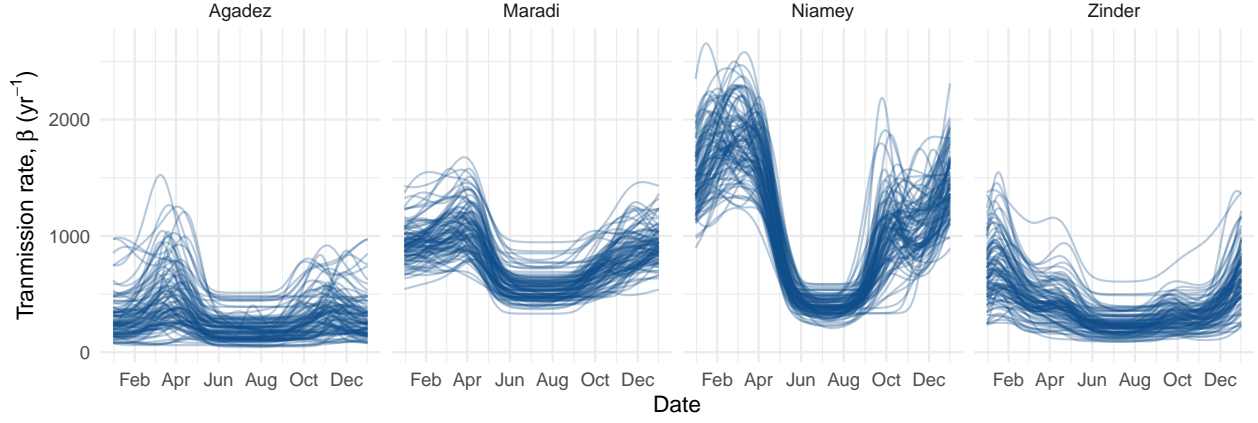
Figure S7: Bootstrap replicates of estimated seasonal transmission functions.

S9. Length of null and test intervals

In the main text we show EWS performance across the range of susceptible discounting factors and vaccination campaign speeds we modeled. To put these values into context, here we show the corresponding window sizes for each simulation. These window sizes are the number of weeks that occur in the null and test intervals (Figure S8).
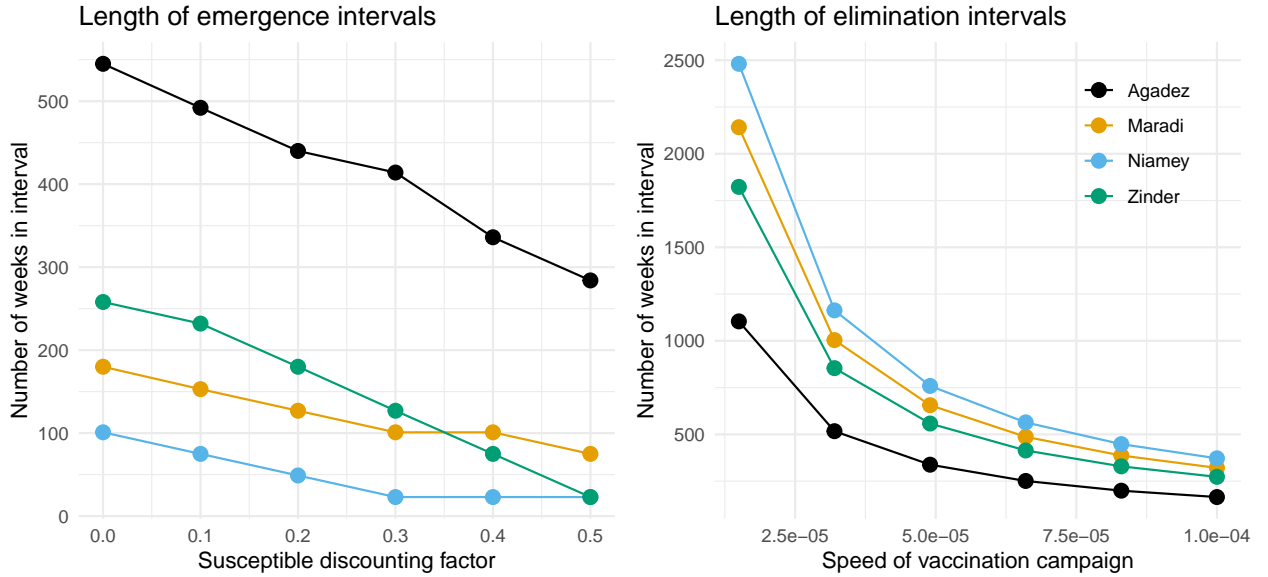

Figure S8: Length of null and test intervals (in weeks) for emergence and elimination simulations at different parameter values.

S10. Moving window analysis

To complement our fixed window analysis presented in the main text, we conducted a moving window analysis as might be conducted on real surveilance data. We used the same null and test intervals as described above for the emergence and elimination scenarios. However, instead of calculating a single value for each EWS over the entire window of the interval, we calculated EWS in the intervals over moving windows of 35 weeks. We then calculated

the Kendall's rank correlation (τ) between each EWS and time in each of the null and test intervals. We used the distributions of Kendall's τ over the 500 replicate simulations to then calculate the Area Under the Curve (AUC) metric for each EWS. For the approach to elimination, the results are similar to those for the fixed window analysis (Figure S9B). For the approach to emergence, however, the moving window results show much worse performance for Agadez and Zinder, and, on average, the AUC values are lower for all EWS in each city (Figure S9A).

(a) **Anticipating emergence over a moving window**

Level of susceptible depletion

(b) **Anticipating elimination over a moving window**
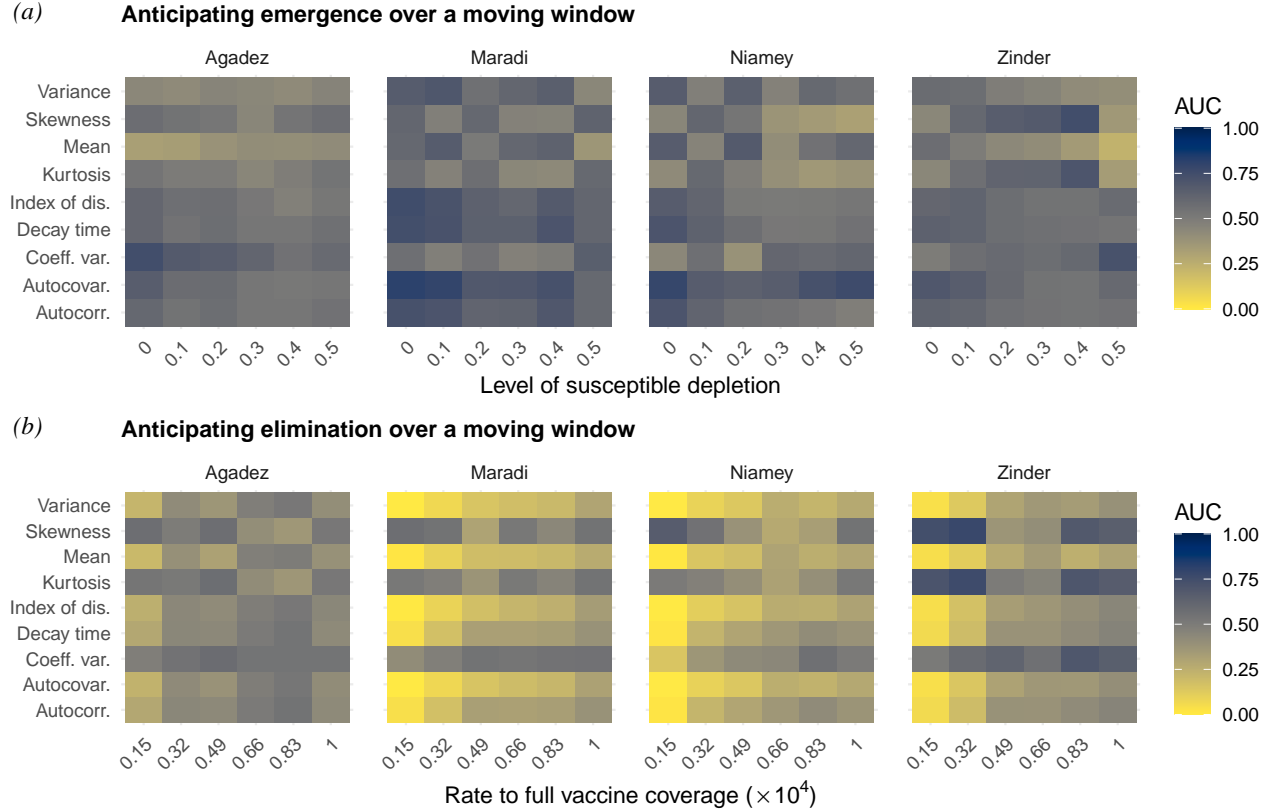

Rate to full vaccine coverage ($\times 10^4$)

Figure S9: Performance of early warning signals (EWS) over a moving window. Correlations between EWS (calculated over 35 week moving windows) and time were calculated over two intervals, one far from a critical transition and one near, for simulations of re-emergence (*a*) and elimination (*b*). EWS performance is quantified using the AUC metric, which we show here as a heatmap of AUC values. AUC values farther from 0.5 indicate higher ability to distinguish among time series near and far from a critical transition.

S11. Susceptible depletion after outbreaks

We *a priori* defined the magnitude of susceptible depletion in our models of measles re-emergence after an outbreak. Thus, a potential limit to our study is that the actual magnitudes of susceptible depletion are less than the values we modeled. That is, maybe we modeled very unrealistic levels of susceptible depletion, making our results interesting but not useful. To test the importance of this limitation, we calculated the relative decline of the susceptible class after outbreak years. We used the 100 replicate simulations that were used for parametric bootstrapping. These simulations adequately reproduce the general dynamics of measles in each city, including outbreak size. We used the simulations because the replicates gave us more outbreaks to work with than the observed data alone.

For each of the 100 replicates for each city, we defined an "outbreak year" as any year in which the cumulative number of reported cases exceeded 80% of the maximum number of cumulative cases observed across all years. We then calculated susceptible depletion (i.e., the susceptible discounting fraction used in our modeling study) as the minimum number of susceptible individuals in the outbreak year divided by the maximum number of susceptible individuals in

the previous year. For example, let year t be an outbreak year where the cumulative number of cases exceeded 80% of the maximum cumulative cases observed. The level of susceptible depletion between year $t-1$ and year t is then: $\min(S_t)/\max(S_{t-1})$. Essentially, this metric tells us the discounting fraction that would need to be applied to S to simulate an outbreak of the size in year t. Histograms for each city are in Figure S10.
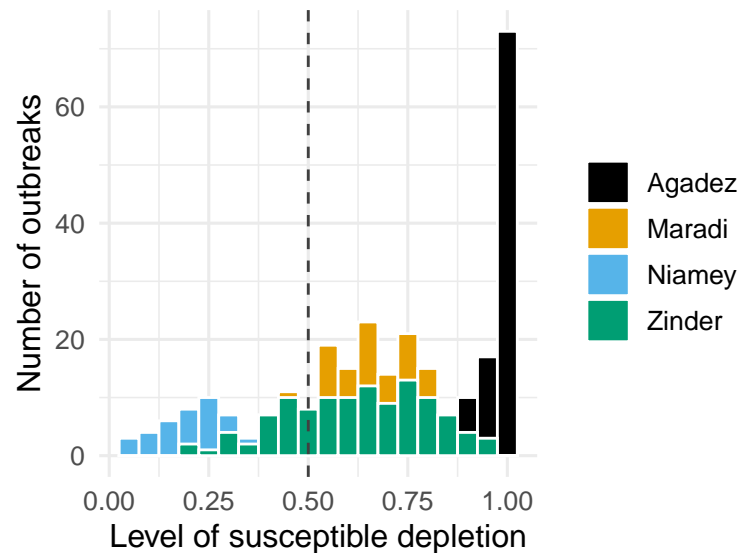

Figure S10: Histograms of susceptible depletion discounting factors for each city. Values were calculated by comparing the number of susceptible individuals before and after large outbreaks from 100 replicate simulations from the fitted models for each city.

References

1. Bretó C, Ionides EL. 2011 Compound Markov counting processes and their applications to modeling infinitesimally over-dispersed systems. *Stochastic Processes and their Applications* **121**, 2571–2591. (doi:10.1016/j.spa.2011.07.005)

2. King AA, Nguyen D, Ionides EL. 2016 Statistical Inference for Partially Observed Markov Processes via the R Package pomp. *Journal Of Statistical Software* **69**, 1–43. (doi:10.18637/jss.v069.i12)

3. King AA *et al.* 2018 pomp: Statistical Inference for Partially Observed Markov Processes (R package, version 1.18).

4. Brett TS, O'Dea EB, Marty É, Miller PB, Park AW, Drake JM, Rohani P. 2018 Anticipating epidemic transitions with imperfect data. *PLoS Computational Biology* **14**, e1006204. (doi:10.1371/journal.pcbi.1006204)